ORIGINAL ARTICLE

# Elevated temperatures accelerate the formation of toxic amyloid fibrils of hen egg-white lysozyme

Zili Feng | Ying Li | Yu Bai 🆔

School of Biological Science and Engineering, Shaanxi University of Technology, Hanzhong, P.R. China

**Correspondence**
Yu Bai, School of Biological Science and Engineering, Shaanxi University of Technology, Hanzhong 723000, P.R. China.
Email: baiu@snut.edu.cn

## Abstract

The formation of amyloid fibrils is critical for neurodegenerative diseases. Some physiochemical conditions can promote the conversion of proteins from soluble globular shapes into insoluble well-organized amyloid fibrils. The aim of this study was to investigate the effect of temperatures on amyloid fibrils formation in vitro using the protein model of hen egg-white lysozyme (HEWL). The HEWL fibrils were prepared at temperatures of 37, 45, 50 and 57°C in glycine solution of pH 2.2. Under transmission electron microscopy, we found the well-organized HEWL amyloid fibrils at temperatures of 45, 50 and 57°C after 10 days of incubation. Thioflavin T and Congo red florescence assays confirmed that the formation and growth of HEWL fibrils displayed a temperature-dependent increase, and 57°C produced the most amounts. Meanwhile, the surface hydrophobicity of aggregates was greatly increased by ANS binding assay, and $\beta$-sheet contents by circular dichroism analysis were increased by 17.8%, 22.0% and 34.9%, respectively. Furthermore, the HEWL fibrils formed at 57°C caused significant cytotoxicity in SH-SY5Y cells after 48 hr exposure, and the cell viability determined by MTT assay was decreased, with 81.35 ± 0.29% for 1 μM, 61.45 ± 2.62% for 2 μM, and 11.58 ± 0.39% ($p < .01$) for 3 μM. Nuclear staining results also confirmed the apoptosis features. These results suggest that the elevated temperatures could accelerate protein unfolding of the native structure and formation of toxic amyloid fibrils, which can improve understanding the mechanisms of the unfolding and misfolding process of prion protein.

**KEYWORDS**
amyloid fibrils, elevated temperatures, hen egg-white lysozyme, prion, protein unfolding

## 1 | INTRODUCTION

The misfolding of the prion protein and amyloid fibrils formation are responsible for animal transmissible spongiform encephalopathies (TSE), also named as prion diseases (Jaunmuktane & Brandner, 2020; Wang et al., 2010), including bovine spongiform encephalopathy (BSE), scrapie of sheep or goat, and chronic wasting disease of deer (Greenlee, 2019; Moreno & Telling, 2018). The self-assembly of prion amyloid fibrils is accompanied by the exposure of hydrophobic patches and conformational change from $\alpha$-helix into $\beta$-sheet of the protein. Prion amyloid fibrils can cause neurons death in vivo and exert neuronal cytotoxicity in primary

neurons or human neuroblastoma SH-SY5Ycells in vitro (Morte et al., 2011).

Human lysozymes with point mutations (e.g., I56T, D67H; Pepys et al., 1993; Booth et al., 1997), and p. Leu102Ser (Nasr et al., 2017) can form into amyloid fibrils which are critical for human familiar amyloidotic disease. Normal human lysozymes can form into amyloid fibrils at physiological pH 7.4 at high temperature of 57℃ (De Felice et al., 2004). The wild-type of hen egg-white lysozyme (HEWL) that is not associated with amyloid-related diseases can also form into similar amyloid fibrils in vitro when exposed to partially denaturing conditions (Krebs et al., 2000). HEWL amyloid fibrils and prion fibrils share common morphology and ultrastructure, and they have identical biochemical properties including long-unbranched fibrils with an axis in the center, enriched $\beta$-sheet structures, and increased surface hydrophobicity (Feng et al., 2012; Wang et al., 2020). Various physiochemical conditions have been reported to induce the formation of HEWL fibrils, such as HCl solution of pH 1.6–pH 2.0 at 65°C (Feng et al., 2012; Ow & Dunstan, 2013), glycine solution of pH 2.2 at 57°C (Mahdavimehr et al., 2017). In addition, metal ions such as $Cu^{2+}$ in solution of pH 7.0 at 60°C (Bhattacharya et al., 2013) and $Al^{3+}$ in solution of pH 2.0 at 60°C (Wawer et al., 2019) can promote HEWL fibrillation. The surfactants like sarkosyl in solution of pH 9.0 (Khan et al., 2018) and sodium dodecyl benzenesulfonate in solution of pH 7.4 (Khan et al., 2019), and food colouring agent like Allura red in solution of pH 7.0 (Al-Shabib et al., 2019) can also promote the formation of HEWL fibrils. Like HEWL protein, prion protein can form into amyloid fibrils under acidic pH conditions demonstrated both by experimental studies (Hornemann & Glockshuber, 1998; Singh & Udgaonkar, 2016) and molecular dynamics simulation techniques (Thompson et al., 2018). Elevated temperatures can accelerate the unfolding process and increase the $\beta$-sheet structures of prion protein using molecular dynamics simulation techniques (Chen et al., 2013; Gu et al., 2003). Hence, HEWL protein and prion protein have similar aggregation-influencing factors like lower pH and higher temperatures.

The α-helix secondary structure can influence the protein aggregation (Steckmann et al., 2012; Wang & Roberts, 2018). HEWL protein contains 129 amino acids. Native HEWL is structurally α-helix rich and has about 40% α-helices as measured by FTIR (Ow & Dunstan, 2013; Sethuraman & Belfort, 2005). Normal prion protein contains about 42% α-helices and the conformational change of prion protein from α-helix into $\beta$-sheet is essential to the formation of prion protein fibrils (Pan et al., 1993). Thus, the similarities in morphological ultrastructure of their fibrils and α-helix-rich structure, as well as in the amyloidogenicity depending on the physiochemical conditions make HEWL protein becoming a good protein model to investigate the mechanisms of prion protein unfolding and amyloid fibril formation in vitro (Buell et al., 2011; Sharma et al., 2016; Swaminathan et al., 2011).

Temperatures influence the protein aggregation process (Wang & Roberts, 2018). Many molecular dynamics simulation studies have previously indicated that the different higher temperatures could accelerate the unfolding process and increase the $\beta$-sheet structures of prion protein by the same mechanisms (Chen et al., 2013; Lee & Chang, 2019). However, due to the inoperability of infectious prion protein, little experimental research has investigated the effect of higher temperatures on the formation of prion amyloid fibrils. Hence, the objective of this study was to investigate the effect of high temperatures on the formation of amyloid fibrils using the protein model of HEWL. Previous studies have demonstrated that HEWL protein could form into amyloid fibrils at 54°C in 50 mM glycine of pH 2.2 (Seraj et al., 2019), 60°C in NaCl and KCl solution of pH 2.0 (Marino et al., 2015), and 65°C in 500 mM glycine of pH 2.0 (Sivalingam et al., 2016). All these previously reported higher temperatures used to generate HEWL amyloid fibrils are specific. However, few studies have been conducted on how elevated temperatures (over physiological 37°C) affected the formation of HEWL amyloid fibrils at lower pH. The influences of 55°C or higher temperatures on the formation of HEWL amyloid fibrils in HCl solution of pH 1.6–2.0 have been reported (Arnaudov & de Vries, 2005; Ow & Dunstan, 2013). We here investigated the effect of physiological 37°C and the higher temperatures of 45, 50 and 57°C on the formation of HEWL amyloid fibrils in 50 mM glycine solution of pH 2.2. We also assessed the neuronal cytotoxicity of the HEWL amyloid fibrils formed at higher temperatures in SH-SY5Y cells, which was aimed to confirm that HEWL protein and prion protein had the similar amyloid fibrils formation mechanisms induced by the elevated temperatures. This study helps to understand the mechanisms by which the elevated temperature affects the protein unfolding and amyloid fibrils formation of prion protein.

## 2 | MATERIALS AND METHODS

### 2.1 | Reagents

HEWL (EC 3.2.1.17) and ThT dye were purchased from Shanghai Haoyuan Chemexpress Co., Ltd. ANS (8-anilino-1-naphthalenesulfonic acid) dye was purchased from Sigma. Congo red dye was purchased from Beijing Solarbio Science & Technology Co., Ltd. The 200-mesh Formvar film-coated copper grids were purchased from Beijing Zhongjingkeyi Technology Co., Ltd. MEM, F-12, Gluta-max, sodium pyruvate, non-essential amino acids (NEAA) and foetal bovine serum were all purchased from Gibco. MTT and Hoechst 33324 were both purchased from Sango Biotech. All other chemicals were biological-reagent grade.

### 2.2 | Amyloid fibrils formation

The purity of HEWL protein was tested using 4%–12% SDS-PAGE and Coomassie blue staining methods. HEWL amyloid fibrils were obtained as previously reported (Mahdavimehr et al., 2017), with minor modifications. HEWL protein was dissolved in 50 mM glycine solution of pH 2.2 to a final concentration of 100 μM. The aliquots

were respectively incubated at 37, 45, 50, and 57°C and agitated at 250 rpm to produce amyloid fibril formation.

## 2.3 | Transmission electron microscopy

After 10 days of incubation at different temperatures, 20 μl of HEWL samples were collected and dropped onto the surface of 200-mesh Formvar film-coated copper grids, negatively stained with phosphotungstic acid (PTA) for 30 s, and air-dried at room temperature. The morphology of HEWL amyloid fibrils was observed under T12 transmission electron microscopy (conducted in the Fourth Military Medical University of China) with voltage of 100 kV.

## 2.4 | ThT fluorescence assay

A ThT fluorescence assay is widely used to measure the formation and growth of amyloid fibrils (Khurana et al., 2005), which is indicated by increased ThT fluorescence intensity. After incubation at the specific temperatures, 40 μl of HEWL samples were diluted in Milli-Q (Shanghai Molecular Instrument Co., Ltd) water to a final concentration of 2 μM and then mixed with 20 μl of ThT stock solution (1 mM) to a final ThT concentration of 10 μM. After incubation for three minutes at room temperature, all ThT fluorescence measurements were conducted on a Cary Eclipse fluorescence spectrophotometer. Upon excitation at 440 nm, fluorescence emission spectra were recorded between 450 and 600 nm, with excitation and emission slit widths both at 5 nm.

## 2.5 | Congo red dye binding assay

Congo red dye binding assay was also used to monitor the formation of amyloid fibrils. The binding of Congo red dye to amyloid fibrils induces a characteristic red shift of maximum absorbance wavelength from 490 to 510 nm and a second shoulder peak around 540 nm(Ma et al., 2017). Congo red dye solution was mixed with incubated HEWL samples to reach a 2:1 concentration ratio of Congo red dye to protein samples. After incubation for 30 min at room temperature, all absorbance spectra were recorded between 400 and 700 nm on a BioTek Microplate Reader, with step length of 10 nm.

## 2.6 | ANS dye binding assay

ANS dye is widely used to detect exposed hydrophobic patches of aggregated proteins (Huang et al., 2009). ANS fluorescence intensity will increase significantly when the ANS dye specifically binds to the hydrophobic patches. After diluting 20 μl of incubated HEWL samples in Milli-Q water to a final concentration of 1 μM,

they were mixed with 20 μl of ANS stock solution (1 mM) to a final ANS concentration of 10 μM. After incubation for 3 min at room temperature, all ANS fluorescence measurements were conducted on a Cary Eclipse fluorescence spectrophotometer. Upon excitation at 380 nm, fluorescence emission spectra were recorded between 420 and 600 nm, with excitation and emission slit widths both at 5 nm.

## 2.7 | Circular dichroism analysis

Circular dichroism (CD) analysis measures secondary structural conversion during amyloid aggregation of proteins. A far-ultraviolet CD spectrum with a negative minimum at 208 is mainly characteristic of $\alpha$-helix conformation, and a negative minimum at 218 nm is mainly characteristic of $\beta$-sheet conformation according to the measurement of ellipticity (Jayamani & Shanmugam, 2014), meanwhile estimated $\beta$-sheet content was measured using BeStSel software (Micsonai et al., 2015). Incubated HEWL samples were diluted in Milli-Q water to a final concentration of 0.1 mg/ml and then immediately subjected to CD measurements on a J-1500 spectropolarimeter (JASCO). Far-ultraviolet CD spectra were recorded between 260 and 190 nm in a quartz cuvette with a 0.1-cm path length. The bandwidth was 1 nm, the scanning speed was 500 nm/min, and six scans were accumulated. The baseline spectrum was subtracted for all spectra.

## 2.8 | Cell culture

Human neuroblastoma SH-SY5Y cells were cultured in complete MEM/F12 medium, containing 1% (v/v) Gluta-max, 1% (v/v) sodium pyruvate, 1% (v/v) NEAA, 10% (v/v) foetal bovine serum, 1% streptomycin (100μg/ml) and penicillin (100 U/ml). The cells were cultured in a 5% $CO_2$ humidified atmosphere at 37°C. Growth medium was changed every 48 hr.

## 2.9 | MTT and nuclear staining analysis

SH-SY5Y cells were seeded in a 96-well plate at a density of $4 \times 10^3$ cells/well. After 24 hr incubation, the cells were exposed to HEWL amyloid fibrils. For cytotoxicity evaluation, the HEWL amyloid fibrils were obtained from 57°C sample. The aggregated fibrils were lyophilized and re-dissolved into the culture medium to final concentrations of 1, 2 and 3 μM. Equivalent concentration of glycine buffer (pH 2.2) was used as control. After treatment for 48 hr, cell apoptosis was determined by MTT and nuclear staining methods. For MTT assay, according to the instruction of MTT kit, 10 μl of MTT stock solutions (5 mg/ml) were added to 90 μl of complete MEM/F12 medium, followed by incubation for 4 hr at 37°C in the dark. Subsequently, the formazan solubilization solution was added and agitated slightly for 10 min to dissolve

the precipitation, followed by absorbance reading at 570 nm on a BioTek Microplate Reader. Cell viability data were expressed as optical density (OD) value according to the following equation: $OD_{treatment}/OD_{control}*100\%$.

For nuclear staining, cultured cells were exposed to 2 and 3 μM HEWL amyloid fibrils for 48 hr separately. Subsequently, the treated cells were stained with Hoechst 33324 for 20 min at room temperature in the dark. Finally, cell nucleus was visualized under an inverted fluorescent microscope (Nikon Ti-S).

## 2.10 | Statistical analysis

Data are presented as the mean ± *SEM* from five replicates. All data were processed using GraphPad prism software (version 5.0). A *t* test and one-way analysis of variance were used to determine the differences among different treatments. $p < .05$ and $p < .01$ were considered statistically significant.

## 3 | RESULTS

### 3.1 | TEM observation

The purity of native HEWL protein was confirmed by SDS-PAGE analysis (Figure S1). The morphological features under TEM gave direct observation of the forming process of amyloid fibrils. We incubated 100 μM HEWL proteins at various temperatures in glycine solution of pH 2.2 for 10 days. Morphological features from TEM results showed that the physiological 37°C samples produced very few and shorter fibrils without rigid axes in the centre, but abundant spherical or rod-shaped aggregated proteins appeared, which showed trends of protein unfolding (Figure 1a). The 45°C samples produced obvious long-unbranched fibrils with straight and rigid axes in the centre, and even some fibrils formed bundles in the field of vision (Figure 1b). The 50°C samples produced a few more fibrils (Figure 1c) than the 45°C samples, and the morphology and ultrastructure are nearly identical. The 57°C samples showed about 5-fold more fibrils in the field of vision than the 50°C samples, displaying mainly more shorter fibrils with identical morphology and diameter (Figure 1d). The amount of formed amyloid fibrils observed in TEM images was gradually increased with the rising temperature.

### 3.2 | ThT fluorescence

The formation and growth of amyloid fibrils was monitored by Thioflavin T dye fluorescence. The fluorescence intensity of ThT dye could enhance significantly when specifically binding to the amyloid fibrils, and we obtained a maximum ThT fluorescence intensity at 482 nm in our experiments. We observed significantly increased ThT fluorescence intensity for the 45, 50, and 57°C samples after 10 days of incubation. The maximal ThT fluorescence

intensity at 482 nm was increased as the temperature elevated from 45 to 57°C ($p <.01$), and the 57°C samples showed the greatest fluorescence intensity (Figure 2a), which coincided with the results of TEM observation. In addition, the ThT fluorescence intensity for the 45–57°C samples also displayed a time-dependent increase when incubated for 10 days (Figure 2b), indicating the continuous growth of HEWL fibrils as incubation progressed. Whereas the 37°C sample showed no obvious increase in ThT fluorescence intensity.

### 3.3 | Congo red analysis

Congo red binding assay was used to probe the presence of a *β*-sheet structure and was widely employed to monitor the formation and growth of HEWL amyloid fibrils. The maximal absorbance appeared around 490 nm for the control sample (native HEWL protein without incubation). We confirmed the characteristic signals of formed *β*-sheet in the 45–57°C samples, displaying a significant red shift from 490 to 510 nm and an obvious shoulder peak around 540 nm. Red shift and shoulder peak were both gradually increased as temperatures elevated from 45 to 57°C (Figure 2c). Whereas the 37°C sample showed neither red shift from 490 to 510 nm nor a shoulder peak around 540 nm, which was identical to the results of TEM observation and ThT fluorescence intensity. These results demonstrated that elevated temperatures (45–57°C) induced the formation and growth of amyloid fibrils after 10 days of incubation.

### 3.4 | ANS binding studies

An ANS binding assay was performed to monitor the hydrophobic patches exposure of protein during aggregation. For 37°C sample, the maximal ANS fluorescence intensity at 482 nm was slightly increased as compared with the control sample, indicating the onset of exposure of hydrophobic patches, although no fibrils were detected either by ThT fluorescence or Congo red binding methods. The maximal ANS fluorescence intensity at 482 nm was gradually increased as temperature elevated from 45 to 50°C. The 57°C sample also showed increased ANS fluorescence intensity, whereas relatively less than the 50°C sample (Figure 2d).

### 3.5 | CD spectra results

The incubated samples were measured for CD spectra at 260–190 nm. According to the measurement of residue ellipticity, no conformational change was detected for 37°C sample, with a major negative minimum appeared at around 208 nm, which was similar with the control. As the temperatures elevated from 45 to 57°C, the amounts of negative minima at around 218 nm were gradually increased (Figure 3), and the corresponding *β*-sheet content estimated by BeStSel software was 23.7%, 27.9% and 40.8%, respectively.
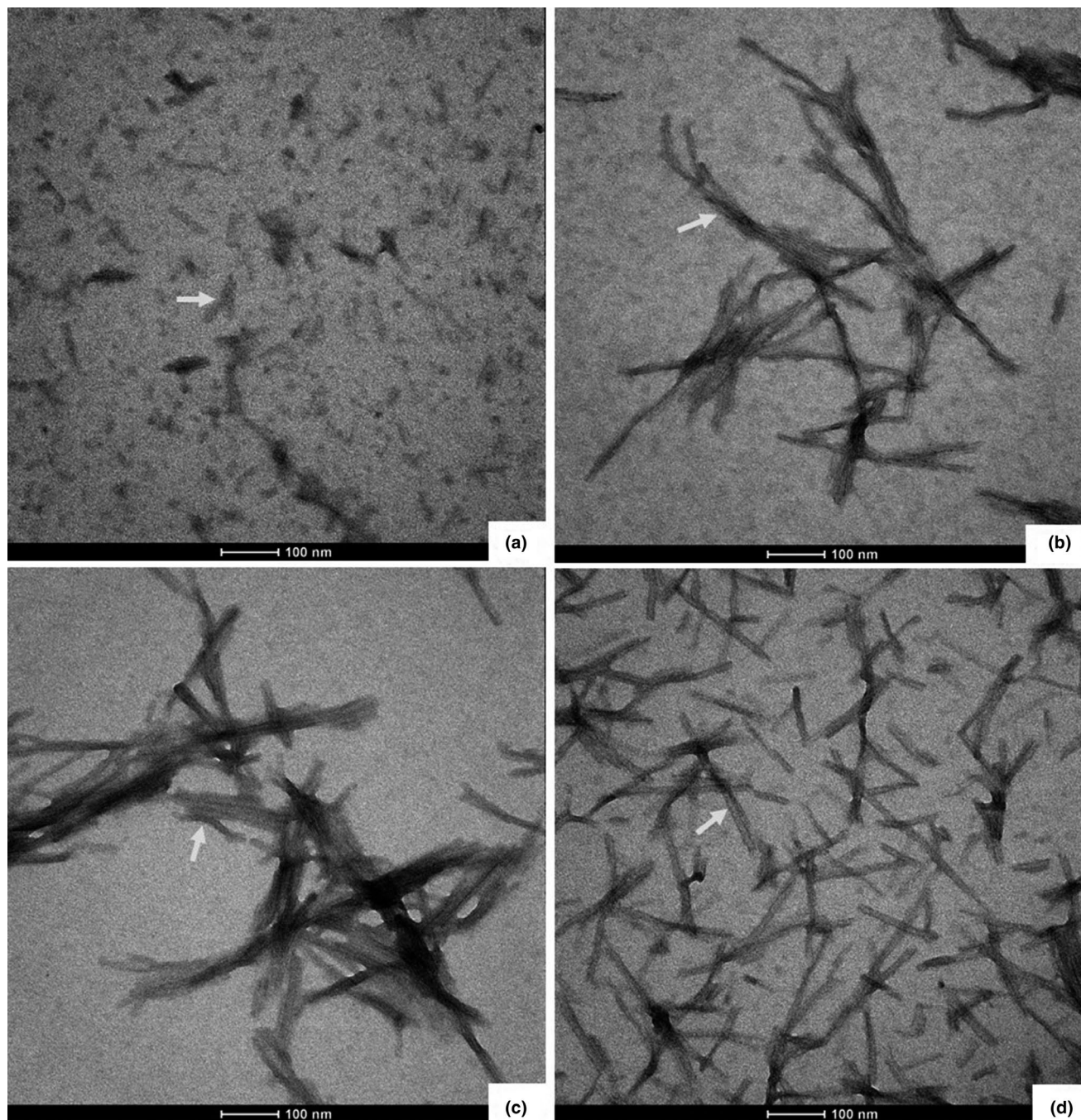
**FIGURE 1** Different temperatures induced morphology of HEWL amyloid fibrils. The morphological ultrastructure was obtained after 10 days of incubation using transmission electron microscopy: (a) 37℃. (b) 45℃. (c) 50℃. (d) 57℃. White arrows indicate the spherical or rod-shaped aggregated proteins or amyloid fibrils. The magnification was indicated

Compared with the control of 5.9%, the $\beta$-sheet contents were gradually increased by 17.8% for 45°C, 22.0% for 50°C and 34.9% for 57°C.

### 3.6 | Cytotoxicity on SH-SY5Y cells

To investigate the cytotoxicity of HEWL fibrils obtained at elevated temperatures, MTT and nuclear staining analysis were conducted on cultured human SH-SY5Y cells. The amyloid fibrils added into the cells were obtained from 57°C samples incubated for 10 days, because 57°C samples produced large amounts of fibrils under the same condition. The MTT results showed that the formed HEWL amyloid fibrils induced marked cytotoxicity after 48 hr exposure (Figure 4). The cell viabilities were $81.35 \pm 0.29\%$ for 1 μM, $61.45 \pm 2.62\%$ for 2 μM, and $11.58 \pm 0.39\%$ ($p < .01$) for 3 μM, which indicated that the pro-apoptotic effect of HEWL fibrils displayed a concentration-dependent manner. While no cytotoxicity was detected for glycine buffer treatment.
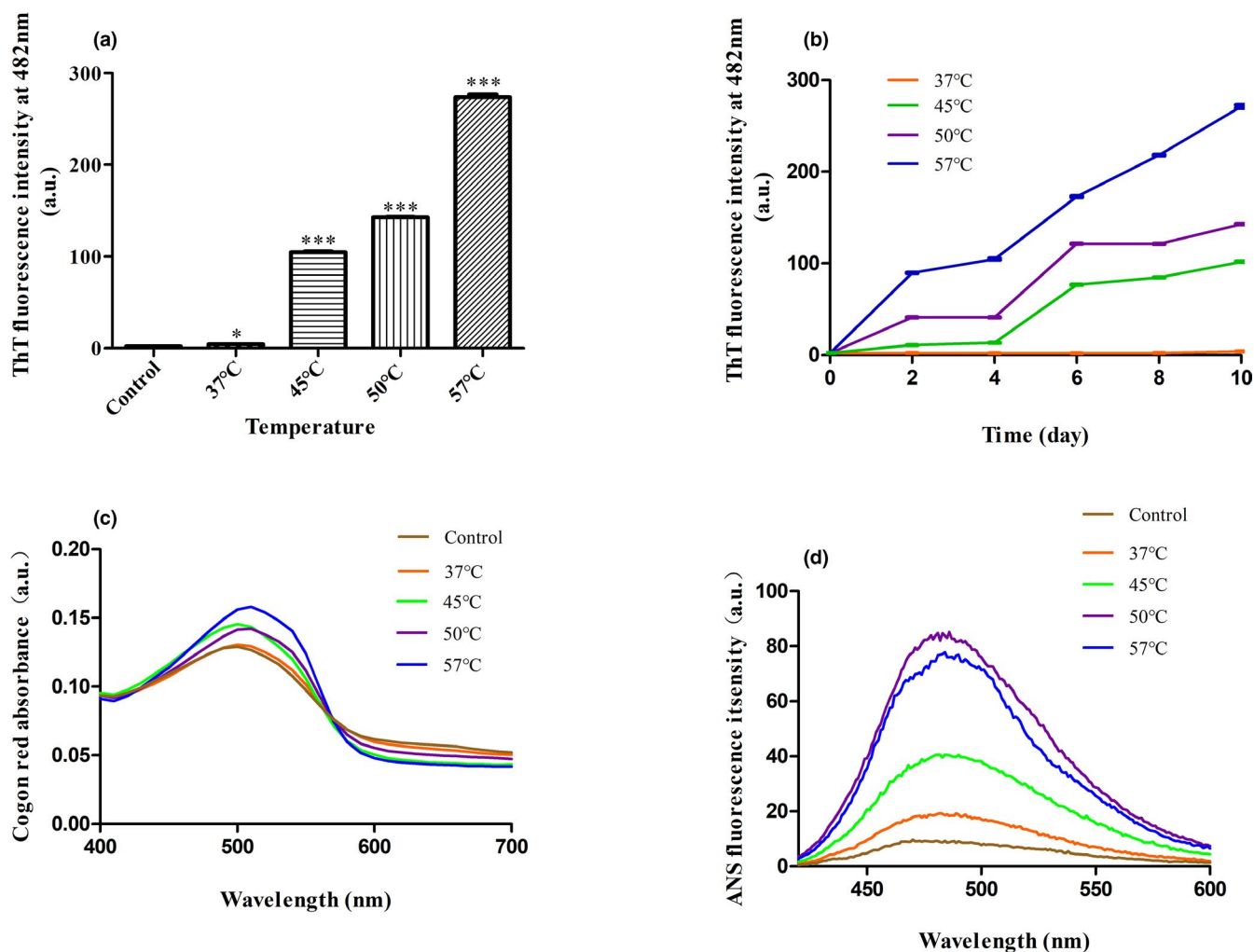
**FIGURE 2** Elevated temperatures induced formation and growth of HEWL amyloid fibrils. (a) ThT fluorescence intensity at 482 nm after 10 days of incubation at 37, 45, 50, and 57°C, respectively (*$p > .05$ vs. control; ***$p < .01$ vs. control). Control indicated native HEWL protein. (b) ThT fluorescence intensity at 482 nm for all samples during different incubation stages. (c) Congo red binding absorbance spectra after 10 days of incubation at 37, 45, 50, and 57°C, respectively. The maximal absorbance was 490 nm for the control and 37°C sample. (d) The maximal ANS fluorescence intensity at 482 nm for all samples. Experimental data represents the mean ± SEM ($n = 5$)
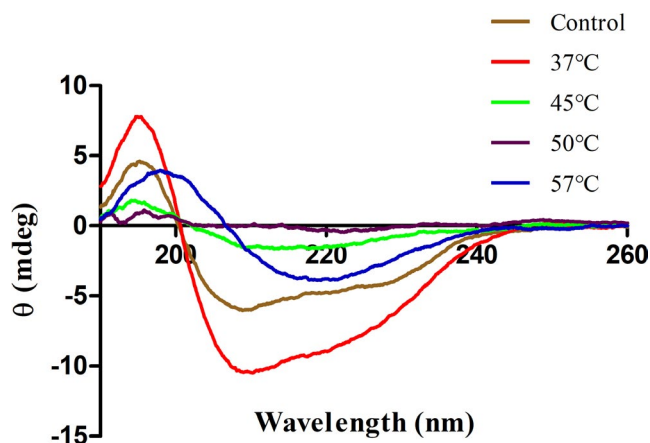


**FIGURE 3** Elevated temperatures induced the conformational change. Far-ultraviolet CD spectra (190–260 nm) analysis for the control and 37–50°C incubated HEWL samples. A major negative minimum at 208 nm represented a predominant α-helical structure, and a major negative minimum at around 218 nm represented a predominant β-sheet structure. θ represents residue ellipticity. Experimental data represents the mean ± SEM ($n = 5$)

Meanwhile, nuclear staining was performed on the cultured cells to evaluate the morphological changes in nuclei. Nuclear staining results showed that 2 μM (Figure 5c) and 3 μM treatments (Figure 5d) with HEWL fibrils both caused marked apoptosis features, including nuclear condensation, nuclear fragmentation, increased brightness, as well as a reduce in the number of cells compared with the control cells, especially 3 μM treatments produced more severe apoptosis features. Neither control (Figure 5a) nor glycine buffer treatment (Figure 5b) induced morphologic changes in nuclei.

## 4 | DISCUSSION

HEWL is well-known for its antibacterial activity. Lysozyme is chosen to study the amyloidogenicity of a globular protein because lysozyme is a well-characterized monomeric globular protein at lower pH related to the amyloidogenicity at high temperatures (Buell et al., 2011; Sharma et al., 2016). HEWL incubated at physiological 37°C produced nearly no visible amyloid fibrils after 10 days
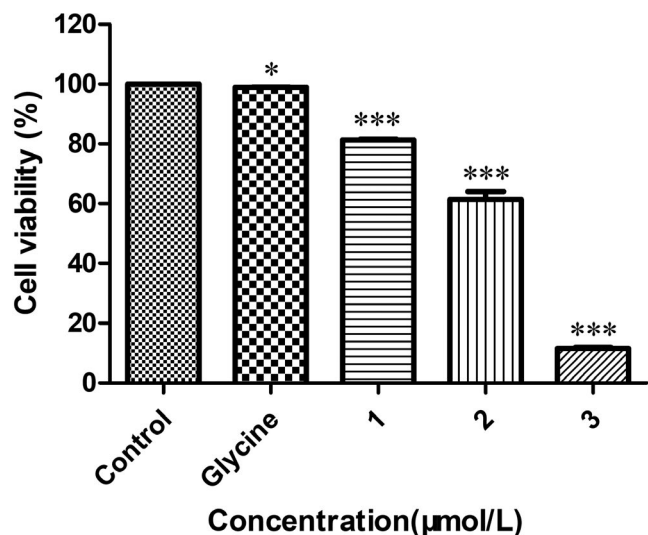
**FIGURE 4** Cell viability in human SH-SY5Y cells caused by HEWL fibrils from 57°C samples Cells were treated with fibrils (1–3 μM) for 48 hr. MTT was used to determine the cell viability (%). *$p > .05$ versus control; ***$p < .01$ versus control. Data are expressed as the mean $\pm$ SEM ($n = 5$)

of incubation in 50 mM glycine solution of pH 2.2. However, the appearance of abundant spherical or rod-shaped aggregates under TEM and the slight exposure of hydrophobic patches by ANS binding assay indicated the initial occurrence of protein unfolding process. If the incubation periods were extended, HEWL protein would probably generate the obvious amyloid fibrils. Our data demonstrated that the formation of HEWL fibrils at physiological 37°C was a slow process, which was in accordance with the evidence that in vivo conversion from PrP$^C$ (cellular prion protein) into pathogenic PrP$^{Sc}$ (scrapie isoform of prion protein) is a gradual process. Large amounts of amyloid fibrils were produced when temperatures were elevated to 45–57°C. Importantly, the TEM ultrastructure of HEWL amyloid fibrils formed at 45–57°C were similar with prion amyloid fibrils (Cavaliere et al., 2013; Wang et al., 2020) or A$\beta$ fibrils(Qiang et al., 2017), all displaying morphology of long-unbranched fibrils with straight and rigid axes in the centre. Amyloid aggregates can display polymorphism, and different environmental conditions may cause diverse morphology of HEWL fibrils(Fujiwara et al., 2003; Ghosh et al., 2015). Previous study has obtained the very long, thin, and straight HEWL fibrils at 57°C or over in HCl solution of pH 2.0 (Arnaudov & de Vries, 2005), but we observed the short rod-shaped morphology of HEWL amyloid fibrils at 45–57°C in 50 mM glycine solution of pH 2.2, even we found that different incubation periods generated different morphology of HEWL fibrils (data not shown). Yeast prion amyloid fibrils also displayed strain-specific morphological differences (Diaz-Avalos et al., 2005). Furthermore, another study generated similar HEWL fibrils at 45, 50 and 55°C in solution of pH 3.8 containing NaCl by crystallization methods (Sharma et al., 2016), although the solution and pH conditions used were totally different from our study. This suggest that elevated temperatures play a key

role in the formation of HEWL amyloid fibrils among the diverse environmental conditions.

The elevated temperatures increased the formation and growth of HEWL amyloid fibrils. ThT fluorescence and Congo red binding assays are the common methods used to quantitively detect the formation and growth of amyloid fibrils in vitro. According to the results of ThT fluorescence intensity, we detected significantly increased growth of fibrils for 45–57°C samples after 10 days of incubation, and the time-dependent growth patterns displayed the same nucleated polymerization mechanism as previously reported (Mahdavimehr et al., 2017). Likewise, the HEWL amyloid fibrils produced at higher temperature also exhibited higher Congo red bindings.

All the evaluated temperatures induced the exposure of hydrophobic patches of HEWL protein after 10 days of incubation. The 37°C samples induced a little higher hydrophobicity compared with the control sample, indicating the initial occurrence of protein unfolding process. The samples from 45, 50 and 57°C all induced more higher hydrophobicity, with more hydrophobicity at 50°C than at 45°C, whereas hydrophobicity at 57°C relatively less than at 50°C. This observation was identical with the results that the environmental conditions induced more HEWL aggregates did not constantly showed higher ANS fluorescence intensity (Brudar & Hribar-Lee, 2019; Sivalingam et al., 2016). The reason might be the loss of hydrophobic patches during elongation of the fibrils at 57°C. It might also be the case that the formation and growth of HEWL amyloid fibrils does not only depend on hydrophobicity (Shih et al., 1995), although hydrophobicity could drive the onset of protein unfolding.

To investigate whether elevated temperatures induced conformational change, a CD spectrum analysis was performed. We found that elevated temperatures increased $\beta$-sheet structures by 17.8% for 45°C, 22.0% for 50°C, and 34.9% for 57°C. The 45–57°C samples significantly increased the unfolding process during aggregation. This was identical to the results using molecular dynamics simulation techniques that elevating temperature could accelerate the unfolding process of prion protein and increase the $\beta$-sheet structures (Chamachi & Chakrabarty, 2017; Chen et al., 2013). Our data were also in accordance with the molecular dynamics simulation results that the structural conversion of cellular prion protein was triggered by acidic pH (Lu et al., 2013; Thompson et al., 2018).

The neuronal cytotoxicity of formed HEWL fibrils at elevated temperatures was assessed in human SH-SY5Y cells. The neuronal cytotoxicity caused by the HEWL fibrils produced at 57°C showed a concentration-dependent increase. The pathological changes of nuclei displayed characteristic apoptosis in accordance with the cytotoxicity caused by prion fibrils. This suggested that HEWL fibrils and prion fibrils contained the similar toxic $\beta$-sheet conformations. The pro-apoptotic effect of HEWL fibrils on human SH-SY5Y cells further proved that HEWL could be a reliable protein model to investigate the mechanism of unfolding process of infectious prion protein.
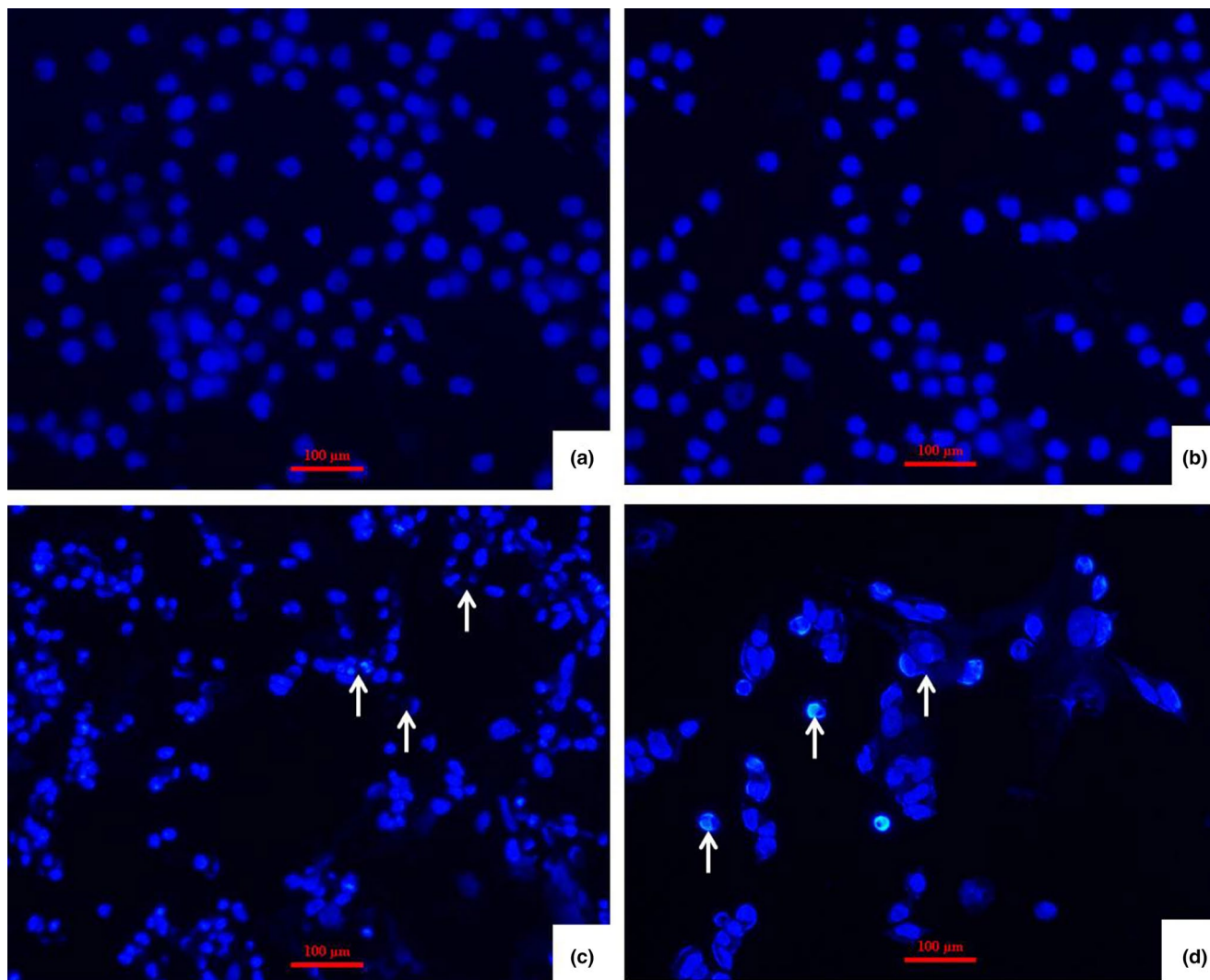
**FIGURE 5** Morphological Changes in nuclei induced by HEWL fibrils from 57°C samples. (a) Control cells stained with Hoechst 33324 and visualized under a fluorescent microscope. (b) Glycine buffer treatment. (c) 2 μM treatments with HEWL fibrils for 48 hr. The reduce in the number of cells was observed compared with control cells. (d) 3 μM treatments with HEWL fibrils for 48 hr. The less cell numbers were observed. White arrows indicated the apoptosis features such as increased brightness, nuclear condensation and nuclear fragmentation. The magnification was indicated

## 5 | CONCLUSIONS

In the present study, the elevated temperatures (over physiological 37°C) ranging from 45 to 57°C greatly were found to accelerate the formation and growth of HEWL amyloid fibrils with neuronal cytotoxicity in SH-SY5Y cells. Our results suggest that high temperatures can easily lead to the exposure of hydrophobic patches and unfolding of the protein monomers, and subsequently facilitate protein unfolding and produce the toxic $\beta$-sheet conformations. We could probably speculate that the neuronal cytotoxicity of amyloid fibrils depends on the nature of self-assembly of proteins, not only on the sequence of proteins. HEWL protein could be a reliable protein model to mimic infectious prion protein for the study of the mechanisms of amyloid fibrils formation. Importantly, temperature plays a key role in the unfolding process during HEWL protein aggregation, which has great significance in understanding the mechanisms of amyloid fibrils formation of infectious prion protein.

## CONFLICT OF INTEREST

The authors declare that they have no conflict of interest.

## AUTHOR CONTRIBUTION

**Zili Feng:** Methodology; Resources; Validation; Writing-original draft. **Ying Li:** Data curation; Investigation; Methodology; Software;

**PEER REVIEW**

The peer review history for this article is available at https://publons.com/publon/10.1002/vms3.522.

**ORCID**

*Yu Bai* 🔟 https://orcid.org/0000-0002-1617-7711

**REFERENCES**

Al-Shabib, N. A., Khan, J. M., Malik, A., Sen, P., Ramireddy, S., Chinnappan, S., Alamery, S. F., Husain, F. M., Ahmad, A., Choudhry, H., Khan, M. I., & Shahzad, S. A. (2019). Allura red rapidly induces amyloid-like fibril formation in hen egg white lysozyme at physiological pH. *International Journal of Biological Macromolecules*, 127, 297–305.

Arnaudov, L. N., & de Vries, R. (2005). Thermally induced fibrillar aggregation of hen egg white lysozyme. *Biophysical Journal*, 88(1), 515–526. https://doi.org/10.1529/biophysj.104.048819

Bhattacharya, S., Ghosh, S., Dasgupta, S., & Roy, A. (2013). Structural differences between native Hen egg white lysozyme and its fibrils under different environmental conditions. *Spectrochimica Acta, Part A: Molecular and Biomolecular Spectroscopy*, 114, 368–376.

Booth, D. R., Sunde, M., Bellotti, V., Robinson, C. V., Hutchinson, W. L., Fraser, P. E., Hawkins, P. N., Dobson, C. M., Radford, S. E., Blake, C. C., & Pepys, M. B. (1997). Instability, unfolding and aggregation of human lysozyme variants underlying amyloid fibrillogenesis. *Nature*, 385(6619), 787–793. https://doi.org/10.1038/385787a0

Brudar, S., & Hribar-Lee, B. (2019). The role of buffers in wild-type HEWL amyloid fibril formation mechanism. *Biomolecules*, 9(2). https://doi.org/10.3390/biom9020065

Buell, A. K., Dhulesia, A., Mossuto, M. F., Cremades, N., Kumita, J. R., Dumoulin, M., Welland, M. E., Knowles, T. P. J., Salvatella, X., & Dobson, C. M. (2011). Population of nonnative states of lysozyme variants drives amyloid fibril formation. *Journal of the American Chemical Society*, 133(20), 7737–7743. https://doi.org/10.1021/ja109620d

Cavaliere, P., Torrent, J., Prigent, S., Granata, V., Pauwels, K., Pastore, A., Rezaei, H., & Zagari, A. (2013). Binding of methylene blue to a surface cleft inhibits the oligomerization and fibrillization of prion protein. *Biochimica et Biophysica Acta*, 1832(1), 20–28. https://doi.org/10.1016/j.bbadis.2012.09.005

Chamachi, N. G., & Chakrabarty, S. (2017). Temperature-induced misfolding in prion protein: evidence of multiple partially disordered states stabilized by non-native hydrogen bonds. *Biochemistry*, 56(6), 833–844. https://doi.org/10.1021/acs.biochem.6b01042

Chen, X., Duan, D., Zhu, S., & Zhang, J. (2013). Molecular dynamics simulation of temperature induced unfolding of animal prion protein. *Journal of Molecular Modeling*, 19(10), 4433–4441. https://doi.org/10.1007/s00894-013-1955-0

De Felice, F. G., Vieira, M. N., Meirelles, M. N., Morozova-Roche, L. A., Dobson, C. M., & Ferreira, S. T. (2004). Formation of amyloid aggregates from human lysozyme and its disease-associated variants using hydrostatic pressure. *The FASEB Journal*, 18(10), 1099–1101. https://doi.org/10.1096/fj.03-1072fje

Diaz-Avalos, R., King, C. Y., Wall, J., Simon, M., & Caspar, D. L. (2005). Strain-specific morphologies of yeast prion amyloid fibrils. *Proceedings of the National Academy of Sciences of the United States of America*, 102(29), 10165–10170. https://doi.org/10.1073/pnas.0504599102

Feng, S., Song, X. H., & Zeng, C. M. (2012). Inhibition of amyloid fibrillation of lysozyme by phenolic compounds involves quinoprotein formation.

*FEBS Letters*, 586(22), 3951–3955. https://doi.org/10.1016/j.febslet.2012.09.037

Fujiwara, S., Matsumoto, F., & Yonezawa, Y. (2003). Effects of salt concentration on association of the amyloid protofilaments of hen egg white lysozyme studied by time-resolved neutron scattering. *Journal of Molecular Biology*, 331(1), 21–28. https://doi.org/10.1016/S0022-2836(03)00722-8

Ghosh, S., Pandey, N. K., Banerjee, P., Chaudhury, K., Nagy, N. V., & Dasgupta, S. (2015). Copper(II) directs formation of toxic amorphous aggregates resulting in inhibition of hen egg white lysozyme fibrillation under alkaline salt-mediated conditions. *Journal of Biomolecular Structure & Dynamics*, 33(5), 991–1007. https://doi.org/10.1080/07391102.2014.921864

Greenlee, J. J. (2019). Review: Update on classical and atypical scrapie in sheep and goats. *Veterinary Pathology*, 56(1), 6–16. https://doi.org/10.1177/0300985818794247

Gu, W., Wang, T., Zhu, J., Shi, Y., & Liu, H. (2003). Molecular dynamics simulation of the unfolding of the human prion protein domain under low pH and high temperature conditions. *Biophysical Chemistry*, 104(1), 79–94. https://doi.org/10.1016/S0301-4622(02)00340-X

Hornemann, S., & Glockshuber, R. (1998). A scrapie-like unfolding intermediate of the prion protein domain PrP(121–231) induced by acidic pH. *Proceedings of the National Academy of Sciences of the United States of America*, 95(11), 6010–6014. https://doi.org/10.1073/pnas.95.11.6010

Huang, B., He, J., Ren, J., Yan, X. Y., & Zeng, C. M. (2009). Cellular membrane disruption by amyloid fibrils involved intermolecular disulfide cross-linking. *Biochemistry*, 48(25), 5794–5800. https://doi.org/10.1021/bi900219c

Jaunmuktane, Z., & Brandner, S. (2020). Invited review: The role of prion-like mechanisms in neurodegenerative diseases. *Neuropathology and Applied Neurobiology*, 46(6), 522–545. https://doi.org/10.1111/nan.12592

Jayamani, J., & Shanmugam, G. (2014). Gallic acid, one of the components in many plant tissues, is a potential inhibitor for insulin amyloid fibril formation. *European Journal of Medicinal Chemistry*, 85, 352–358.

Khan, J. M., Khan, M. S., Alsenaidy, M. A., Ahmed, A., Sen, P., Oves, M., Al-Shabib, N. A., & Khan, R. H. (2018). Sodium louroyl sarcosinate (sarkosyl) modulate amyloid fibril formation in hen egg white lysozyme (HEWL) at alkaline pH: A molecular insight study. *Journal of Biomolecular Structure & Dynamics*, 36(6), 1550–1565. https://doi.org/10.1080/07391102.2017.1329097

Khan, J. M., Malik, A., Sen, P., Ahmed, A., Ahmed, M., Alamery, S. F., Almaharfi, H. A., Choudhry, H., & Khan, M. I. (2019). Different conformational states of hen egg white lysozyme formed by exposure to the surfactant of sodium dodecyl benzenesulfonate. *International Journal of Biological Macromolecules*, 128, 54–60.

Khurana, R., Coleman, C., Ionescu-Zanetti, C., Carter, S. A., Krishna, V., Grover, R. K., Roy, R., & Singh, S. (2005). Mechanism of thioflavin T binding to amyloid fibrils. *Journal of Structural Biology*, 151(3), 229–238. https://doi.org/10.1016/j.jsb.2005.06.006

Krebs, M. R., Wilkins, D. K., Chung, E. W., Pitkeathly, M. C., Chamberlain, A. K., Zurdo, J., Robinson, C. V., & Dobson, C. M. (2000). Formation and seeding of amyloid fibrils from wild-type hen lysozyme and a peptide fragment from the beta-domain. *Journal of Molecular Biology*, 300(3), 541–549.

Lee, J., & Chang, I. (2019). Structural insight into conformational change in prion protein by breakage of electrostatic network around H187 due to its protonation. *Scientific Reports*, 9(1), 19305.

Lu, X., Zeng, J., Gao, Y., Zhang, J. Z., Zhang, D., & Mei, Y. (2013). The intrinsic helical propensities of the helical fragments in prion protein under neutral and low pH conditions: A replica exchange molecular dynamics study. *Journal of Molecular Modeling*, 19(11), 4897–4908. https://doi.org/10.1007/s00894-013-1985-7

Ma, B., Zhang, F., Wang, X., & Zhu, X. (2017). Investigating the inhibitory effects of zinc ions on amyloid fibril formation of hen egg-white

lysozyme. *International Journal of Biological Macromolecules*, *98*, 717–722.

Mahdavimehr, M., Meratan, A. A., Ghobeh, M., Ghasemi, A., Saboury, A. A., & Nemat-Gorgani, M. (2017). Inhibition of HEWL fibril formation by taxifolin: Mechanism of action. *PLoS One*, *12*(11), e0187841.

Marino, L., Pauwels, K., Casasnovas, R., Sanchis, P., Vilanova, B., Munoz, F., Donoso, J., & Adrover, M. (2015). Ortho-methylated 3-hydroxypyridines hinder hen egg-white lysozyme fibrillogenesis. *Scientific Reports*, *5*, 12052.

Micsonai, A., Wien, F., Kernya, L., Lee, Y. H., Goto, Y., Refregiers, M., & Kardos, J. (2015). Accurate secondary structure prediction and fold recognition for circular dichroism spectroscopy. *Proceedings of the National Academy of Sciences of the United States of America*, *112*(24), E3095–3103.

Moreno, J. A., & Telling, G. C. (2018). Molecular mechanisms of chronic wasting disease prion propagation. *Cold Spring Harbor Perspectives in Medicine*, *8*(6). https://doi.org/10.1101/cshperspect.a024448

Morte, B., Martínez, T., Zambrano, A., & Pascual, A. (2011). Monocyte-mediated regulation of genes by the amyloid and prion peptides in SH-SY5Y neuroblastoma cells. *Neurochemistry International*, *58*(6), 613–619. https://doi.org/10.1016/j.neuint.2011.01.019

Nasr, S. H., Dasari, S., Mills, J. R., Theis, J. D., Zimmermann, M. T., Fonseca, R., Vrana, J. A., Lester, S. J., McLaughlin, B. M., Gillespie, R., Highsmith, W. E. Jr, Lee, J. J., Dispenzieri, A., & Kurtin, P. J. (2017). Hereditary lysozyme amyloidosis variant p.Leu102Ser associates with unique phenotype. *Journal of the American Society of Nephrology*, *28*(2), 431–438. https://doi.org/10.1681/ASN.2016090951

Ow, S. Y., & Dunstan, D. E. (2013). The effect of concentration, temperature and stirring on hen egg white lysozyme amyloid formation. *Soft Matter*, *9*(40), 9692–9701. https://doi.org/10.1039/c3sm51671g

Pan, K. M., Baldwin, M., Nguyen, J., Gasset, M., Serban, A., Groth, D., Mehlhorn, I., Huang, Z., Fletterick, R. J., & Cohen, F. E. (1993). Conversion of alpha-helices into beta-sheets features in the formation of the scrapie prion proteins. *Proceedings of the National Academy of Sciences of the United States of America*, *90*(23), 10962–10966. https://doi.org/10.1073/pnas.90.23.10962

Pepys, M. B., Hawkins, P. N., Booth, D. R., Vigushin, D. M., Tennent, G. A., Soutar, A. K., Totty, N., Nguyen, O., Blake, C. C. F., Terry, C. J., Feest, T. G., Zalin, A. M., & Hsuan, J. J. (1993). Human lysozyme gene mutations cause hereditary systemic amyloidosis. *Nature*, *362*(6420), 553–557. https://doi.org/10.1038/362553a0

Qiang, W., Yau, W. M., Lu, J. X., Collinge, J., & Tycko, R. (2017). Structural variation in amyloid-β fibrils from Alzheimer's disease clinical subtypes. *Nature*, *541*(7636), 217–221. https://doi.org/10.1038/nature20814

Seraj, Z., Groves, M. R., & Seyedarabi, A. (2019). Cinnamaldehyde and Phenyl Ethyl Alcohol promote the entrapment of intermediate species of HEWL, as revealed by structural, kinetics and thermal stability studies. *Scientific Reports*, *9*(1), 18615.

Sethuraman, A., & Belfort, G. (2005). Protein structural perturbation and aggregation on homogeneous surfaces. *Biophysical Journal*, *88*(2), 1322–1333. https://doi.org/10.1529/biophysj.104.051797

Sharma, P., Verma, N., Singh, P. K., Korpole, S., & Ashish (2016). Characterization of heat induced spherulites of lysozyme reveals new insight on amyloid initiation. *Scientific Reports*, *6*, 22475.

Shih, P., Holland, D. R., & Kirsch, J. F. (1995). Thermal stability determinants of chicken egg-white lysozyme core mutants: Hydrophobicity, packing volume, and conserved buried water molecules. *Protein Science*, *4*(10), 2050–2062. https://doi.org/10.1002/pro.5560041010

Singh, J., & Udgaonkar, J. B. (2016). Unraveling the molecular mechanism of pH-induced misfolding and oligomerization of the prion protein. *Journal of Molecular Biology*, *428*(6), 1345–1355. https://doi.org/10.1016/j.jmb.2016.01.030

Sivalingam, V., Prasanna, N. L., Sharma, N., Prasad, A., & Patel, B. K. (2016). Wild-type hen egg white lysozyme aggregation in vitro can form self-seeding amyloid conformational variants. *Biophysical Chemistry*, *219*, 28–37.

Steckmann, T., Awan, Z., Gerstman, B. S., & Chapagain, P. P. (2012). Kinetics of peptide secondary structure conversion during amyloid β-protein fibrillogenesis. *Journal of Theoretical Biology*, *301*, 95–102.

Swaminathan, R., Ravi, V. K., Kumar, S., Kumar, M. V., & Chandra, N. (2011). Lysozyme: A model protein for amyloid research. *Advances in Protein Chemistry and Structural Biology*, *84*, 63–111.

Thompson, H. N., Thompson, C. E., Andrade Caceres, R., Dardenne, L. E., Netz, P. A., & Stassen, H. (2018). Prion protein conversion triggered by acidic condition: A molecular dynamics study through different force fields. *Journal of Computational Chemistry*, *39*(24), 2000–2011. https://doi.org/10.1002/jcc.25380

Wang, G., Zhou, X., Bai, Y., Zhang, Z., & Zhao, D. (2010). Cellular prion protein released on exosomes from macrophages binds to Hsp70. *Acta Biochimica et Biophysica Sinica*, *42*(5), 345–350. https://doi.org/10.1093/abbs/gmq028

Wang, L. Q., Zhao, K., Yuan, H. Y., Wang, Q., Guan, Z., Tao, J., Li, X. N., Sun, Y., Yi, C. W., Chen, J., Li, D., Zhang, D., Yin, P., Liu, C., & Liang, Y. (2020). Cryo-EM structure of an amyloid fibril formed by full-length human prion protein. *Nature Structural & Molecular Biology*, *27*(6), 598–602. https://doi.org/10.1038/s41594-020-0441-5

Wang, W., & Roberts, C. J. (2018). Protein aggregation – Mechanisms, detection, and control. *International Journal of Pharmaceutics*, *550*(1–2), 251–268.

Wawer, J., Szocinski, M., Olszewski, M., Piatek, R., Naczk, M., & Krakowiak, J. (2019). Influence of the ionic strength on the amyloid fibrillogenesis of hen egg white lysozyme. *International Journal of Biological Macromolecules*, *121*, 63–70.

## SUPPORTING INFORMATION

Additional supporting information may be found online in the Supporting Information section.